WestVirginiaUniversity
THE RESEARCH REPOSITORY @ WVU

Faculty Scholarship

2018

Electron paramagnetic resonance and optical absorption study of acceptors in CdSiP2 crystals

E M. Scherrer

L E. Halliburton

E M. Golden

K T. Zawilski

P G. Schunemann

See next page for additional authors

Authors

E M. Scherrer, L E. Halliburton, E M. Golden, K T. Zawilski, P G. Schunemann, F K. Hopkins, K L. Averett, and N C. Giles

Electron paramagnetic resonance and optical absorption study of acceptors in CdSiP$_2$ crystals

E. M. Scherrer, L. E. Halliburton, E. M. Golden, K. T. Zawilski, P. G. Schunemann [ID], F. K. Hopkins, K. L. Averett, and N. C. Giles

ARTICLES YOU MAY BE INTERESTED IN

Electron paramagnetic resonance and optical absorption study of acceptors in CdSiP$_2$ crystals

E. M. Scherrer,[1] L. E. Halliburton,[2,3] E. M. Golden,[1] K. T. Zawilski,[4] P. G. Schunemann,[4] F. K. Hopkins,[5] K. L. Averett,[5] and N. C. Giles[1,a]

[1]*Department of Engineering Physics, Air Force Institute of Technology, Wright-Patterson Air Force Base, Ohio 45433, USA*
[2]*Department of Physics and Astronomy, West Virginia University, Morgantown, West Virginia 26506, USA*
[3]*Azimuth Corporation, 4027 Colonel Glenn Highway, Suite 230, Beavercreek, Ohio 45431, USA*
[4]*BAE Systems, Nashua, New Hampshire 03061, USA*
[5]*Air Force Research Laboratory, Materials and Manufacturing Directorate, Wright-Patterson Air Force Base, Ohio 45433, USA*

Cadmium silicon diphosphide (CdSiP$_2$) is a nonlinear material often used in optical parametric oscillators (OPOs) to produce tunable laser output in the mid-infrared. Absorption bands associated with donors and acceptors may overlap the pump wavelength and adversely affect the performance of these OPOs. In the present investigation, electron paramagnetic resonance (EPR) is used to identify two unintentionally present acceptors in large CdSiP$_2$ crystals. These are an intrinsic silicon-on-phosphorus antisite and a copper impurity substituting for cadmium. When exposed to 633 nm laser light at temperatures near or below 80 K, they convert to their neutral paramagnetic charge states (Si$_P^0$ and Cu$_{Cd}^0$) and can be monitored with EPR. The corresponding donor serving as the electron trap is the silicon-on-cadmium antisite (Si$_{Cd}^{2+}$ before illumination and Si$_{Cd}^+$ after illumination). Removing the 633 nm light and warming the crystal above 90 K quickly destroys the EPR signals from both acceptors and the associated donor. Broad optical absorption bands peaking near 0.8 and 1.4 μm are also produced at low temperature by the 633 nm light. These absorption bands are associated with the Si$_P^0$ and Cu$_{Cd}^0$ acceptors. © *2018 Author(s). All article content, except where otherwise noted, is licensed under a Creative Commons Attribution (CC BY) license (http://creativecommons.org/licenses/by/4.0/).* https://doi.org/10.1063/1.5041806

I. INTRODUCTION

Cadmium silicon diphosphide (CdSiP$_2$) crystals belong to the tetrahedrally bonded family of chalcopyrite-structured II-IV-V$_2$ semiconducting materials. The nonlinear optical properties of this group of crystals are of special interest, with considerable effort in recent years being focused on applications of CdSiP$_2$.[1–5] When compared to ZnGeP$_2$, the CdSiP$_2$ crystals have a larger direct optical gap (approaching 2.45 eV) and a higher nonlinear optical coefficient (d$_{36}$ = 84.5 pm/V). These favorable properties have encouraged the development of CdSiP$_2$-based optical parametric oscillators (OPOs) that produce tunable laser output in the mid-infrared.[4–9] Pump wavelengths as short as 1.064 μm can generate idler beams near 6 μm in these OPOs.[7] Recently, CdSiP$_2$ crystals have been shown to be efficient generators of terahertz (THz) radiation via optical rectification when pumped with ultrashort near-infrared (50 fs, 780 nm) pulses.[10]

Unintentional donors and acceptors are often found in the II-IV-V$_2$ semiconductors. Their presence nearly always degrades the performance of an OPO by introducing unwanted optical absorption

---

[a]Author to whom correspondence should be addressed: Nancy.Giles@afit.edu

bands that overlap the pump wavelengths. These crystals are usually compensated (with nearly equal concentrations of donors and acceptors), and thus there are few free carriers at room temperature. Exposure to near-band-edge laser light converts these defects to their paramagnetic charge states as electrons move from the acceptors to donors. The high resolution and sensitivity of photoinduced electron paramagnetic resonance (EPR) makes this technique a preferred method to individually monitor the optically active donors and acceptors in bulk II-IV-V$_2$ crystals.[11,12] A series of EPR studies have identified zinc-vacancy acceptors (V_{Zn}^-), phosphorus-vacancy donors (V_P^+), and germanium-on-zinc antisite donors (Ge_{Zn}^+) in ZnGeP$_2$ crystals.[13–17] More recently, in CdSiP$_2$, EPR has been used to identify silicon-vacancy acceptors (V_{Si}^-), cadmium-vacancy acceptors (V_{Cd}^-), and silicon-on-cadmium antisite donors (Si_{Cd}^+).[18,19] Optical studies of CdSiP$_2$ have shown that broad absorption bands, photoinduced at room temperature and peaking near 0.8 and 1.9 μm, are correlated with the presence of silicon vacancies.[20] In addition to a recent computational study[21] of intrinsic point defects in CdSiP$_2$, there have been several computational studies that focused on important non-defect-related properties of CdSiP$_2$.[22–25]

In the present paper, we use photoinduced EPR to identify and characterize two additional acceptors in a CdSiP$_2$ crystal. These are the silicon-on-phosphorus antisite and a copper impurity substituting for cadmium. The new acceptors are present in their nonparamagnetic charge states (Si_P^- and Cu_{Cd}^-) in the as-grown crystal. They are then converted to paramagnetic charge states (Si_P^0 and Cu_{Cd}^0) during an illumination at low temperature with 633 nm laser light. A subsequent exposure to 1064 nm laser light while the crystal continues to be held at low temperature destroys all the photoinduced EPR signals (i.e., the paramagnetic charge states), as the electrons that were temporarily trapped at donors return to acceptors by way of the conduction band. Identifications of the new acceptors are based primarily on the resolved hyperfine structure in their EPR spectra. The thermal stabilities of these neutral charge states are investigated in the 70 to 100 K region. In addition to the EPR spectra, two broad optical absorption bands peaking near 0.8 and 1.4 μm are produced at low temperature during an exposure to 633 nm light. These absorption bands are most likely linked to the presence of the neutral charge states of the two acceptors. Although the neutral acceptors are not thermally stable at room temperature, they may appear in a transient form during the operation of CdSiP$_2$-based optical parametric oscillators, especially when short-wavelength, very intense, pump pulses are used. These near-infrared absorption bands, even though short-lived, could restrict the maximum usable pump power for an OPO, and thus limit the idler output power that is generated in the mid-infrared.

Before proceeding, it is useful to clarify the semiconductor notation being used for the copper acceptor.[26] The Cu_{Cd}^0 label refers to a neutral copper atom that has replaced a neutral cadmium atom in the lattice (this is an A^0 center in semiconductor terms with one unpaired electron, and thus is paramagnetic). The Cu_{Cd}^- label refers to copper that has accepted an extra electron (this is an A^- center in semiconductor terms with no unpaired electrons). The neutral Cu_{Cd}^0 and singly ionized Cu_{Cd}^- acceptors both have a filled $3d^{10}$ shell; they also have either one or two outer electrons, respectively, that are partially delocalized onto neighboring anions and cations. Thus, the Cu_{Cd}^0 defect in CdSiP$_2$ resembles a classic (i.e., hydrogenic) semiconductor acceptor rather than the ionic model of a Cu^{2+} ($3d^9$) ion that has the unpaired spin localized within the 3d shell.

II. EXPERIMENTAL

The undoped CdSiP$_2$ crystal used in this study was grown at BAE Systems (Nashua, NH) using the horizontal gradient freeze method. After being oriented with the x-ray Laue technique, an EPR-sized sample with dimensions of $3 \times 3 \times 5$ mm^3 was cut from the larger as-grown boule. This sample was used to obtain both EPR and optical absorption spectra. The CdSiP$_2$ crystals are tetragonal with space group $I\bar{4}2d$.[27] Reference 19 provides a detailed description of this structure that is useful for point defect studies. As is typical for many CdSiP$_2$ crystals, EPR spectra revealed that our sample contained trace amounts of Mn and Fe ions.[18,19] These impurities came from the starting materials used to grow the crystals. The Si_P^0 and Cu_{Cd}^0 acceptors and the Si_{Cd}^+ donor, the focus of the present investigation, were also observed in additional CdSiP$_2$ crystals recently grown at

BAE Systems. Unlike many earlier-grown $CdSiP_2$ crystals, however, there were few silicon vacancies in these recently grown crystals and thus there was little photoinduced optical absorption at room temperature in the 0.65-2.0 μm region.[20]

A Bruker EMX spectrometer operating near 9.40 GHz was used to take the EPR spectra. Values of the resonant static magnetic fields were measured with a Bruker NMR teslameter and the temperature of the sample was controlled with an Oxford helium-gas flow system. The Cr^{3+} EPR signal from a small MgO crystal (the isotropic g value of the Cr^{3+} ion is 1.9800) was used to correct for the slight difference in magnetic field between the sample and the tip of the teslameter probe. A He-Ne laser (633 nm) and a cw Nd:YAG laser (1.064 μm) were used to produce and destroy the paramagnetic charge states of the new acceptors, respectively. During these illuminations, there was no measurable increase in the temperature of the sample due to absorption of laser light. A ThermoScientific Nicolet 8700 FTIR spectrometer was used to obtain optical absorption spectra in the 0.65 to 2.5 μm region. The white light source was used for all wavelengths, while a silicon detector was used for wavelengths shorter than 1 μm and a DGTS detector was used for longer wavelengths. A cryostat from Cryo Industries (Model 110-637-DND) and a temperature controller from LakeShore (Model 335) were used to take optical absorption data below room temperature.

III. EPR RESULTS

Figure 1(a) shows the EPR spectrum obtained while the $CdSiP_2$ crystal was exposed at 77 K to 633 nm laser light. The magnetic field is along the *c* direction. There were no detectable EPR signals, other than those from the Mn^{2+} ions, before the exposure to laser light. As will be demonstrated in this section, the EPR spectrum in Fig. 1(a) has three contributing paramagnetic defects. These are the photoinduced singly ionized Si-on-Cd antisite donor (Si_{Cd}^+) and two photoinduced neutral acceptors. In previous studies, the Si_{Cd}^+ defects were shown to be the dominant donor in
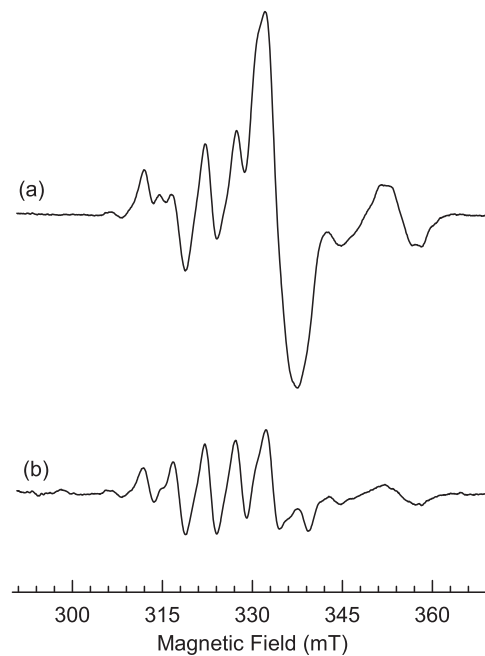

FIG. 1. EPR spectra from an undoped $CdSiP_2$ crystal taken at 77 K and high microwave power. The magnetic field is along the *c* direction in the crystal. (a) The upper trace was acquired during an exposure to 633 nm laser light. Overlapping spectra from the Si_P^0 and Cu_{Cd}^0 acceptors and the Si_{Cd}^+ donor are present. (b) The lower trace was acquired five minutes after the laser light was removed. During the five minutes in the "dark" at 77 K, nearly all of the spectrum from the Si_P^0 acceptor thermally decayed (its primary line is near 333 mT), leaving the spectrum of the Cu_{Cd}^0 acceptor and a portion of the spectrum from the Si_{Cd}^+ donor.

$CdSiP_2$.[19,20] One of the new acceptors is a Cu-on-Cd (Cu_{Cd}^0) and the other is a Si-on-P antisite (Si_P^0). Neither acceptor has been reported in earlier studies of $CdSiP_2$. Exposure to 1064 nm laser light while the crystal continues to be held at low temperature destroys the EPR signals that had been photoinduced with 633 nm light. The 1064 nm light moves electrons from the Si-on-Cd antisite (Si_{Cd}^+) donors to the conduction band. These mobile electrons then recombine with holes trapped at the acceptors.

The three contributing EPR spectra in Fig. 1(a) are strongly overlapping, thus a complex non-symmetrical pattern is produced. A separate spectrum for each defect can be obtained by taking data with and without 633 nm incident light, after selected decay times, and at different microwave powers. The Si_P^0 acceptor is slightly less stable than the Cu_{Cd}^0 acceptor. This allows the Si_P^0 acceptor spectrum to be removed by simply waiting for several minutes at 77 K (after shuttering the 633 nm light), as this charge state thermally decays while leaving nearly all of the spectrum from the Cu_{Cd}^0 acceptor. The spectrum from the Si_{Cd}^+ antisite donor is easily saturated with microwave power, as a result of a long spin-lattice relaxation time. By operating the EPR spectrometer at very low microwave power (as shown in Fig. 2), the other defects are minimized and the Si_{Cd}^+ antisite donor is the primary contributor to the observed spectrum. We observed no photoinduced changes in the intensities of the lines from the Mn^{2+} $(3d^5)$ ions.[18,19,28] Thus, in all the EPR spectra shown here, these lines have been subtracted.

Figure 1(b) shows the EPR spectrum acquired five min after removing the 633 nm laser light. These "light-on" and "light-off" spectra in Fig. 1 were taken at the same temperature and with the same spectrometer settings. The major difference in these two spectra is the absence of the large feature located near 333 mT in the light-off spectrum. This EPR signal, assigned to the neutral Si-on-P acceptor (Si_P^0), thermally decayed during the five min wait in the dark at 77 K. An isolated spectrum of this Si_P^0 acceptor is shown later in Fig. 4(a). Because our EPR spectra are strongly overlapping, we do not attempt in the present study to obtain separate thermal decay curves for individual defects (and thus their activation energies), as has been done in other EPR studies.[29]
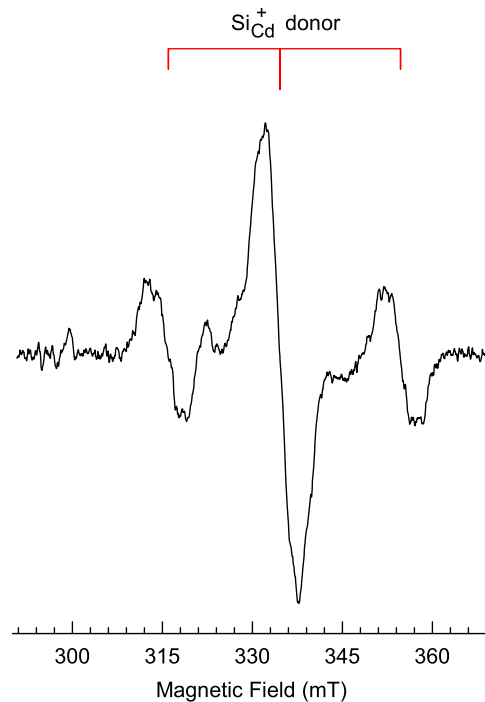
FIG. 2. Three-line EPR spectrum of the Si_{Cd}^+ donor from an undoped $CdSiP_2$ crystal taken at 77 K during an exposure to 633 nm laser light. The magnetic field is parallel to the *c* direction. Low microwave power was used because the Si_{Cd}^+ donor has a long spin-lattice relaxation time, and is easily saturated. There is a small contribution to the middle line from the Si_P^0 acceptor. The low microwave power minimized the signal from the Cu_{Cd}^0 acceptor.

The EPR spectrum in Fig. 2 was taken at very low microwave power and shows primarily the Si-on-Cd antisite donor (Si_{Cd}^+). These data were obtained at 77 K with 633 nm laser light on the crystal. At this low power, the Cu_{Cd}^0 acceptor signals are too weak to observe. The spectrum of the Si_{Cd}^+ donor in Fig. 2 consists of three equally spaced lines, with a 1:2:1 ratio of intensities. Equal hyperfine interactions with two of the four phosphorus ions adjacent to the antisite Si ion are responsible for this three-line pattern.[19] A small contribution from the Si_P^0 acceptor is also present in Fig. 2. Close examination of the spectrum reveals that the middle line in the spectrum is more than twice as intense as the two outer lines, thus providing specific evidence that this line contains a contribution from the Si_P^0 acceptor. Because they are broad and have similar *g* values (near 2.00), the middle line of the Si_{Cd}^+ donor is not easily distinguished from the primary line of the Si_P^0 acceptor.

The isolated spectrum for the neutral Cu_{Cd}^0 acceptor is shown in Fig. 3(a). This spectrum was obtained by subtracting the spectrum in Fig. 2 representing the Si_{Cd}^+ antisite donor from the spectrum in Fig. 1(b) that contains the Cu_{Cd}^0 acceptor and Si_{Cd}^+ donor. An appropriate scaling of the intensity of the spectrum in Fig. 2 was done to ensure its complete removal in Fig. 3(a). After the Si_{Cd}^+ spectrum is removed, the remaining easily seen spectrum is from the Cu_{Cd}^0 acceptor. It consists of eight resolved lines, equally spaced but with varying intensities. The outer two lines on the low and high field sides of the spectrum are significantly less intense than the four lines in the middle. As expected, the EPR spectrum of the Cu_{Cd}^0 acceptor in $CdSiP_2$ in Fig. 3(a) strongly resembles the spectrum previously reported for the neutral Cu_{Zn}^0 acceptor in $ZnGeP_2$.[26] In these chalcopyrite semiconductors, copper behaves as a "classic" acceptor with a filled $3d^{10}$ shell and one or two outer delocalized electrons. This is in direct contrast to the Cu^{2+} ($3d^9$) ions often seen with EPR in more ionic crystals.

As described earlier[26] for the Cu_{Zn}^0 acceptor in $ZnGeP_2$, the hyperfine pattern in the Cu_{Cd}^0 spectrum in Fig. 3(a) is caused by interactions with the central Cu nucleus (either ^{63}Cu or ^{65}Cu) and four
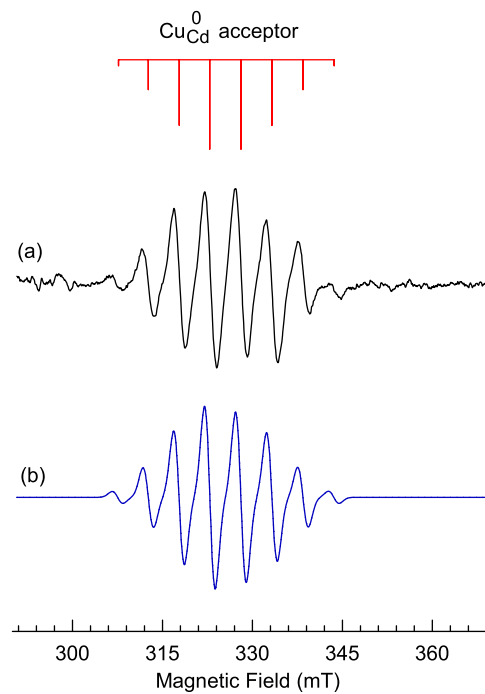

FIG. 3. (a) The EPR spectrum of the neutral Cu_{Cd}^0 acceptor in an undoped $CdSiP_2$ crystal. This is the spectrum that remains after the Si_{Cd}^+ donor and a small contribution from the Si_P^0 acceptor are removed from the spectrum in Fig. 1(b). The stick diagrams above the experimental spectrum illustrate the hyperfine contributions from the ^{63}Cu and ^{65}Cu nuclei and the four neighboring ^{31}P nuclei. (b) The simulated EPR spectrum of the Cu_{Cd}^0 acceptor, produced using the EasySpin computer program.

nearest-neighbor ^{31}P nuclei. The following spin Hamiltonian describes this spin system.

$$H = \beta \mathbf{S} \cdot \mathbf{g} \cdot \mathbf{B} + \mathbf{I}_{Cu} \cdot \mathbf{A}_{Cu} \cdot \mathbf{S} + \sum_{1}^{4} \mathbf{I}_P \cdot \mathbf{A}_P \cdot \mathbf{S} \tag{1}$$

A stick diagram above the spectrum illustrates these hyperfine splittings. The ^{63}Cu and ^{65}Cu isotopes are 69.2% and 30.8% abundant, respectively, with I = 3/2 for both, and the ^{31}P nuclei are 100% abundant with I = 1/2. By themselves, these Cu nuclei will produce a four-line spectrum since the two isotopes have similar nuclear magnetic moments. The additional equal hyperfine interactions with the four adjacent I = 1/2 phosphorous nuclei will split each of these Cu lines into five lines, thus giving a total of 20 lines. Many of the expected 20 lines are directly overlapping and only eight lines are resolved in the experimental spectrum in Fig. 3(a). This reduction from 20 to 8 lines is a direct result of the ^{63,65}Cu and ^{31}P hyperfine interactions being nearly equal in magnitude. The eight observed lines will have intensity ratios of 1:5:11:15:15:11:5:1 if the Cu and P parameters are equal and the small difference in the magnetic moments of the Cu isotopes is ignored. These predicted ratios agree well with the observed line intensities. The four parameters needed to describe the *c*-axis experimental spectrum in Fig. 3(a) are a *g* factor and hyperfine for the central Cu nuclei and the four equivalent neighboring P nuclei. Values for these parameters are g_c = 2.062, $A_c(^{63}Cu)$ = 5.10 mT, $A_c(^{65}Cu)$ = 5.46 mT, and $A_c(^{31}P)$ = 5.10 mT. The simulated spectrum shown in Fig. 3(b) was generated using these values and the open-access EasySpin[30] computer program.

When the magnetic field is along either of the two equivalent *a* directions in the crystal, the EPR spectrum of the neutral Cu_{Cd}^0 acceptor collapses to one broad line with g_a = 2.067 and a width of approximately 5.0 mT. Individual Cu and P hyperfine lines are not resolved. Although values of the $A_a(^{63,65}Cu)$ and $A_a(^{31}P)$ hyperfine parameters cannot be directly obtained from the *a*-direction EPR spectrum, estimates based on the width of the line suggests that these parameters are approximately three to four times smaller than the *c*-direction values.

The final step in the deconvolution of the EPR spectrum in Fig. 1(a) is to extract the isolated spectrum of the Si_P^0 acceptor. Use is made of the five min waiting period that occurred after taking the spectrum in Fig. 1(a) and before taking the spectrum in Fig. 1(b). While the sample was in the dark at 77 K, nearly all the Si_P^0 acceptors and a significant portion of the Si_{Cd}^+ donors thermally decayed. A difference spectrum obtained by subtracting the spectrum in Fig. 1(b) from the spectrum in Fig. 1(a) consists primarily of contributions from the Si_P^0 acceptor and the Si_{Cd}^+ donor. The spectrum from only the Si_P^0 acceptor is then obtained by subtracting the spectrum in Fig. 2, representing primarily the Si_{Cd}^+ donor, from this difference spectrum. Again, an appropriate scaling of the intensity of the spectrum in Fig. 2 was done to ensure the complete removal of the Si_{Cd}^+ donor signals. The resulting EPR spectrum of the neutral Si_P^0 acceptors in $CdSiP_2$, without interference from other spectra, is shown in Fig. 4(a).

The EPR spectrum of the Si_P^0 acceptor in Fig. 4(a) consists of a large center line and two much smaller adjacent hyperfine lines. These weaker lines are symmetrically located about the center line and are not well-resolved. They represent hyperfine interactions with the ^{111}Cd and ^{113}Cd nuclei located at one neighboring Cd site. The following spin Hamiltonian is appropriate.

$$H = \beta \mathbf{S} \cdot \mathbf{g} \cdot \mathbf{B} + \mathbf{I}_{Cd} \cdot \mathbf{A}_{Cd} \cdot \mathbf{S} \tag{2}$$

The ^{111}Cd isotope is 12.8% abundant with I = 1/2 and the ^{113}Cd isotope is 12.2% abundant with I = 1/2. These isotopes have nearly the same magnetic moments. The parameters that describe the Si_P^0 spectrum in Fig. 4(a) are g_c = 2.0077 and $A_c(^{111,113}Cd)$ = 16.9 mT. Here, $A_c(^{111,113}Cd)$ represents an average of the values for the ^{111}Cd and ^{113}Cd nuclei. Using these parameters, a simulated EPR spectrum of the neutral Si_P^0 acceptor was produced with the EasySpin computer program.[30] This simulated spectrum is shown in Fig. 4(b).

The observation of hyperfine lines representing an interaction with nuclei at one neighboring Cd site is consistent with a Si-on-P acceptor. The neutral Si_P^0 acceptor has two nearest-neighbor Cd ions and two nearest-neighbor Si ions, but there is no fundamental requirement that the unpaired spin be delocalized over two or more of these neighboring cations. The ^{29}Si nuclei are only 4.7% abundant with I = 1/2. Hyperfine parameters for a neighboring Si ion are expected to be approximately four times smaller than the parameters for a neighboring Cd ion.[31,32] These smaller parameters, coupled
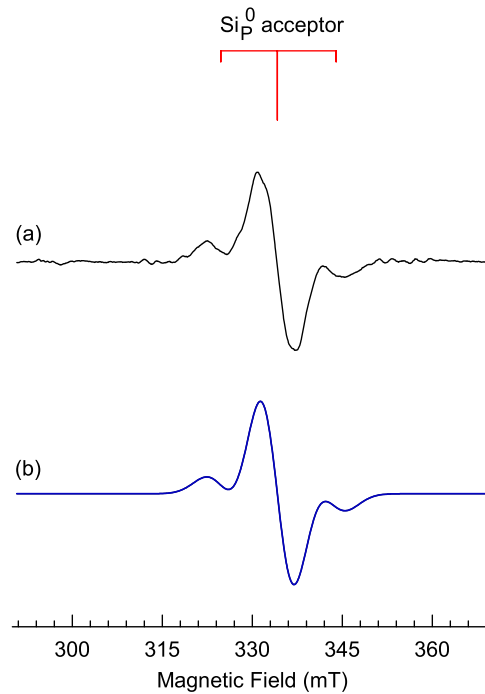
FIG. 4. (a) The EPR spectrum of the neutral Si_P^0 acceptor in an undoped $CdSiP_2$ crystal. This is the spectrum that remains after taking the difference between the spectra in Figs. 1(a) and 1(b) and then subtracting the spectrum in Fig. 2 from the difference spectrum. This latter subtraction removes the Si_{Cd}^+ donor. Stick diagrams above the spectrum illustrate the I = 0 central line and the weaker hyperfine lines from the ^{111}Cd and ^{113}Cd nuclei at one neighboring Cd site. (b) A simulated EPR spectrum of the Si_P^0 acceptor, produced using the EasySpin computer program.

with the smaller natural abundance, suggest that ^{29}Si hyperfine lines from one or more neighboring Si ions will not be resolved in the EPR spectrum of the Si_P^0 acceptor, especially in light of the large linewidths exhibited by this spectrum. This leaves ^{111}Cd and ^{113}Cd as the responsible nuclei for the observed hyperfine interaction in Fig. 4(a). The relative intensities of the central line and the pair of adjacent hyperfine lines in the simulated spectrum in Fig. 4(b) supports this assignment to the ^{111}Cd and ^{113}Cd nuclei located at one neighboring cadmium site.

Acceptors analogous to the Si_P^0 center in $CdSiP_2$ have been studied in other II-IV-V_2 crystals. An EPR spectrum in $CdGeAs_2$, showing resolved hyperfine from ^{111}Cd and ^{113}Cd nuclei, has been assigned to the neutral Ge_{As}^0 acceptor.[33] Subsequent computational modeling verified the assignment of this spectrum to the Ge_{As}^0 acceptor.[34] Recent modeling results[35] for donors and acceptors in $ZnSiP_2$ suggest that singly ionized Si_P^- acceptors will be present in crystals grown in silicon-rich conditions. Exposure to near-band-gap light at low temperature would then convert these Si_P^- acceptors in $ZnSiP_2$ to the neutral Si_P^0 state, provided there are suitable compensating donors such as Si_{Zn}^{2+} available to trap the photo-released electrons and become Si_{Zn}^+ centers. Thus far, there have been no experimental or computational studies of neutral Ge_P^0 antisite acceptors in $ZnGeP_2$ crystals.

IV. OPTICAL ABSORPTION RESULTS

In addition to defect-related EPR spectra, optical absorption bands in the near-infrared region are formed in our $CdSiP_2$ crystal during an exposure to 633 nm laser light while being held at low temperature. Figure 5 shows the absorption spectra taken at various temperatures. The light propagated along the *a* axis of the crystal, the optical path length was 3.0 mm, and corrections for surface reflections were made using published values for the indices of refraction.[1,36] The slight discontinuities in the spectra at 1 µm are caused by the detector change. Spectrum (a) in Fig. 5 was taken at room temperature. The 633 nm light from the He-Ne laser introduced very little near-infrared
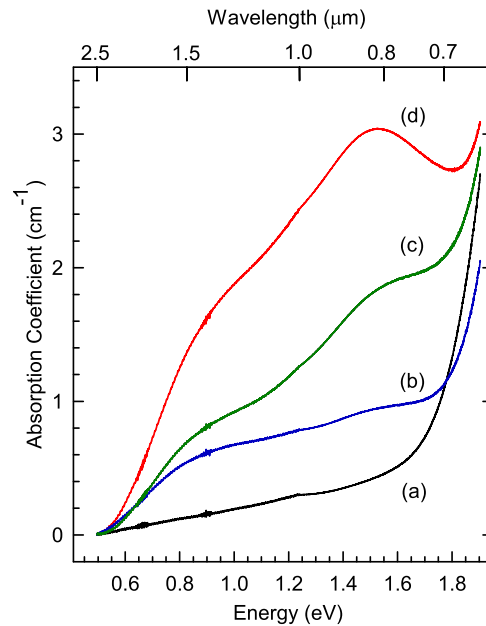
FIG. 5. Optical absorption spectra obtained from an undoped CdSiP$_2$ crystal during exposure to 633 nm laser light. Spectra were taken at (a) room temperature, (b) 150 K, (c) 125 K, and (d) 100 K.

absorption at this temperature. Spectrum (a) remained essentially the same before, during, and after the exposure at room temperature to the laser light. Spectra (b), (c), and (d) in Fig. 5 were taken at 150, 125, and 100 K, respectively, with 633 nm light on the crystal.

In Fig. 5, two broad photoinduced absorption bands, peaking near 0.8 and 1.4 μm, appear and grow as the temperature is lowered. Our EPR results showed a similar production behavior for the neutral Si_P^0 and Cu_{Cd}^0 acceptors, thus leading us to suggest that these acceptors may be associated with the induced absorption bands. Future investigations of CdSiP$_2$ involving polarization, temperature dependence, and different excitation wavelengths are expected to identify the nature of the various optical transitions and thus allow bands to be assigned to specific defects.

V. SUMMARY

Large single crystals of CdSiP$_2$ grown for nonlinear optical applications contain significant concentrations of unintentional donors and acceptors. When these compensated crystals are illuminated at or near 77 K with 633 nm laser light, defects are converted to paramagnetic charge states that can be monitored with EPR. Photoinduced spectra from neutral silicon-on-phosphorus antisites (Si_P^0) and neutral copper impurities substituting for cadmium (Cu_{Cd}^0) are observed and characterized in the present study. The photoinduced paramagnetic donors that accompany these acceptors are silicon-on-cadmium antisites (Si_{Cd}^+). When the light is removed and the crystal is kept near 77 K, the EPR spectrum from the Si_P^0 acceptors thermally decays at a faster rate than the spectrum from the Cu_{Cd}^0 acceptors. This indicates that the Cu_{Cd}^0 acceptors have a deeper 0/− level than the Si_P^0 acceptors. They thermally decay when an electron is thermally excited from the valence band to the neutral acceptor, thus producing a hole in the valence band that then annihilates the electron trapped at the singly ionized donor (Si_{Cd}^+). At low temperature, exposure to 633 nm laser light also produces two broad optical absorption bands with peaks near 0.8 and 1.4 μm. The appearance of these infrared bands coincides with the production of the Si_P^0 and Cu_{Cd}^0 EPR spectra.

ACKNOWLEDGMENTS

[1] K. T. Zawilski, P. G. Schunemann, T. M. Pollak, D. E. Zelmon, N. C. Fernelius, and F. K. Hopkins, "Growth and characterization of large CdSiP$_2$ single crystals," J. Cryst. Growth **312**, 1127 (2010).
[2] V. Petrov, "Frequency down-conversion of solid-state laser sources to the mid-infrared spectral range using non-oxide nonlinear crystals," Prog. Quantum Electron. **42**, 1 (2015).
[3] F. K. Hopkins, S. Guha, B. Claflin, P. G. Schunemann, K. T. Zawilski, N. C. Giles, and L. E. Halliburton, "Potential of CdSiP$_2$ for enabling mid-infrared laser sources," Proc. SPIE **9616**, 96160W (2015).
[4] P. G. Schunemann, K. T. Zawilski, L. A. Pomeranz, D. J. Creeden, and P. A. Budni, "Advances in nonlinear optical crystals for mid-infrared coherent sources," J. Opt. Soc. Am. B **33**, D36 (2016).
[5] C. M. Liebig, F. K. Hopkins, K. L. Averett, K. T. Zawilski, P. G. Schunemann, E. M. Scherrer, N. C. Giles, and L. E. Halliburton, "Status of CdSiP$_2$ development for scaling mid-infrared laser power," Proc. SPIE **10637**, 106370U (2018).
[6] L. Pomeranz, J. McCarthy, R. Day, K. Zawilski, and P. Schunemann, "Efficient, 2-5 μm tunable CdSiP$_2$ optical parametric oscillator pumped by a laser source at 1.57 μm," Opt. Lett. **43**, 130 (2018).
[7] S. Chaitanya Kumar, K. T. Zawilski, P. G. Schunemann, and M. Ebrahim-Zadeh, "High-repetition-rate, deep-infrared, picosecond optical parametric oscillator based on CdSiP$_2$," Opt. Lett. **42**, 3606 (2017).
[8] S. Chaitanya Kumar, P. G. Schunemann, K. T. Zawilski, and M. Ebrahim-Zadeh, "Advances in ultrafast optical parametric sources for the mid-infrared based on CdSiP$_2$," J. Opt. Soc. Am. B **33**, D44 (2016).
[9] S. Chaitanya Kumar, J. Krauth, A. Steinmann, K. T. Zawilski, P. G. Schunemann, H. Giessen, and M. Ebrahim-Zadeh, "High-power femtosecond mid-infrared optical parametric oscillator at 7 μm based on CdSiP$_2$," Opt. Lett. **40**, 1398 (2015).
[10] B. N. Carnio, P. G. Schunemann, K. T. Zawilski, and A. Y. Elezzabi, "Generation of broadband terahertz pulses via optical rectification in a chalcopyrite CdSiP$_2$ crystal," Opt. Lett. **42**, 3920 (2017).
[11] J. A. Weil and J. R. Bolton, *Electron Paramagnetic Resonance: Elementary Theory and Practical Applications*, 2nd ed. (John Wiley and Sons, Hoboken, New Jersey, 2007).
[12] J.-M. Spaeth and H. Overhof, *Point Defects in Semiconductors and Insulators: Determination of Atomic and Electronic Structure from Paramagnetic Hyperfine Interactions* (Springer-Verlag, Berlin, 2003).
[13] M. H. Rakowsky, W. K. Kuhn, W. J. Lauderdale, L. E. Halliburton, G. J. Edwards, M. P. Scripsick, P. G. Schunemann, T. M. Pollak, M. C. Ohmer, and F. K. Hopkins, "Electron paramagnetic resonance study of a native acceptor in as-grown ZnGeP$_2$," Appl. Phys. Lett. **64**, 1615 (1994).
[14] L. E. Halliburton, G. J. Edwards, M. P. Scripsick, M. H. Rakowsky, P. G. Schunemann, and T. M. Pollak, "Electron-nuclear double resonance of the zinc vacancy in ZnGeP$_2$," Appl. Phys. Lett. **66**, 2670 (1995).
[15] N. C. Giles, L. E. Halliburton, P. G. Schunemann, and T. M. Pollak, "Photoinduced electron paramagnetic resonance of the phosphorus vacancy in ZnGeP$_2$," Appl. Phys. Lett. **66**, 1758 (1995).
[16] S. D. Setzler, N. C. Giles, L. E. Halliburton, P. G. Schunemann, and T. M. Pollak, "Electron paramagnetic resonance of a cation antisite defect in ZnGeP$_2$," Appl. Phys. Lett. **74**, 1218 (1999).
[17] W. Gehlhoff, D. Azamat, A. Hoffmann, and N. Dietz, "Structure and energy level of native defects in as-grown and electron-irradiated zinc germanium diphosphide studied by EPR and photo-EPR," J. Phys. Chem. Solids **64**, 1923 (2003).
[18] N. C. Giles, L. E. Halliburton, S. Yang, X. Yang, A. T. Brant, N. C. Fernelius, P. G. Schunemann, and K. T. Zawilski, "Optical and EPR study of point defects in CdSiP$_2$ crystals," J. Cryst. Growth **312**, 1133 (2010).
[19] E. M. Golden, N. C. Giles, E. Maniego, F. K. Hopkins, K. T. Zawilski, P. G. Schunemann, and L. E. Halliburton, "Identification of native defects (vacancies and antisites) in CdSiP$_2$ crystals," J. Appl. Phys. **118**, 185702 (2015).
[20] E. M. Scherrer, B. E. Kananen, E. M. Golden, F. K. Hopkins, K. T. Zawilski, P. G. Schunemann, L. E. Halliburton, and N. C. Giles, "Defect-related optical absorption bands in CdSiP$_2$ crystals," Opt. Mater. Express **7**, 658 (2017).
[21] C. Wang, J. Sun, H. Gou, S. Wang, J. Zhang, and X. Tao, "Intrinsic defects and their effects on the optical properties in the nonlinear optical crystal CdSiP$_2$: A first-principles study," Phys. Chem. Chem. Phys. **19**, 9558 (2017).
[22] W. R. L. Lambrecht and X. Jiang, "Noncritically phase-matched second-harmonic-generation chalcopyrites based on CdSiAs$_2$ and CdSiP$_2$," Phys. Rev. B **70**, 045204 (2004).
[23] Z. L. Lv, H. L. Cui, H. Wang, X. H. Li, and G. F. Ji, "Study of the vibrational, dielectric and infrared properties of CdSiP$_2$ via first principles," Solid State Commun. **246**, 88 (2016).
[24] J. Xiao, Z. He, S. Zhu, B. Chen, and G. Jiang, "Hybrid functional study of structural, electronic, bonding and optical properties of CdSiP$_2$," Comput. Mater. Sci. **117**, 472 (2016).
[25] L. Wei, Y. Zhang, X. Lv, Y. Yang, H. Yu, Y. Hu, H. Zhang, X. Wang, B. Liu, and Q. Li, "Intrinsic sources of high thermal conductivity of CdSiP$_2$ determined by first-principle anharmonic calculations," Phys. Chem. Chem. Phys. **20**, 1568 (2018).
[26] K. T. Stevens, L. E. Halliburton, S. D. Setzler, P. G. Schunemann, and T. M. Pollak, "Electron paramagnetic resonance and electron-nuclear double resonance study of the neutral copper acceptor in ZnGeP$_2$ crystals," J. Phys.: Condens. Matter **15**, 1625 (2003).
[27] S. C. Abrahams and J. L. Bernstein, "Luminescent piezoelectric CdSiP$_2$: Normal probability plot analysis, crystal structure, and generalized structure of the A^{II}B^{IV}C$_2^{V}$ family," J. Chem. Phys. **55**, 796 (1971).
[28] U. Kaufmann, A. Rauber, and J. Schneider, "ESR analysis of IIB-IV-V$_2$ semiconductors with Mn^{2+} as a paramagnetic probe," Phys. Stat. Sol. **74**, 169 (1976).
[29] E. Erdem, "Microwave power, temperature, atmospheric and light dependence of intrinsic defects in ZnO nanoparticles: A study of electron paramagnetic resonance (EPR) spectroscopy," J. Alloys Compd. **605**, 34 (2014).
[30] S. Stoll and A. Schweiger, "EasySpin, a comprehensive software package for spectral simulation and analysis in EPR," J. Magn. Reson. **178**, 42 (2006).
[31] J. R. Morton and K. F. Preston, "Atomic parameters for paramagnetic resonance data," J. Magn. Reson. **30**, 577 (1978).

[32] J. A. J. Fitzpatrick, F. R. Manby, and C. M. Western, "The interpretation of molecular magnetic hyperfine interactions," J. Chem. Phys. **122**, 084312 (2005).

[33] L. Bai, N. Y. Garces, N. Yang, P. G. Schunemann, S. D. Setzler, T. M. Pollak, L. E. Halliburton, and N. C. Giles, "Optical and EPR study of defects in cadmium germanium arsenide," Mat. Res. Soc. Symp. Proc. **744**, 537 (2003).

[34] M. A. Blanco, A. Costales, V. Luaña, and R. Pandey, "Theoretical study of the group-IV antisite acceptor defects in CdGeAs₂," Appl. Phys. Lett. **85**, 4376 (2004).

[35] A. D. Martinez *et al.*, "Solar energy conversion properties and defect physics of ZnSiP₂," Energy Environ. Sci. **9**, 1031 (2016).

[36] J. Wei, J. M. Murray, F. K. Hopkins, D. M. Krein, K. T. Zawilski, P. G. Schunemann, and S. Guha, "Measurement of refractive indices of CdSiP₂ at temperatures from 90 to 450 K," Opt. Mater. Express **8**, 235 (2018).